

Two transient X-ray Quasi-Periodic Oscillations separated by an intermediate state in 1H 0707-495

Peng-Fei Zhang,^{1,2} Peng Zhang,^{1,3} Neng-Hui Liao,¹ Jing-Zhi Yan,^{1,*} Yi-Zhong Fan,^{1,4,†} and Qing-Zhong Liu^{1,4}

¹Key Laboratory of Dark Matter and Space Astronomy,

Purple Mountain Observatory, Chinese Academy of Sciences, Nanjing 210008, China

²Key Laboratory of Astroparticle Physics of Yunnan Province, Yunnan University, Kunming 650091, China

³University of Chinese Academy of Sciences, Beijing, 100012, China

⁴School of Astronomy and Space Science, University of Science and Technology of China, Hefei, Anhui 230026, China

In the narrow-line Seyfert 1 galaxy 1H 0707-495, recently a transient quasi-periodic oscillation (QPO) signal has been detected at a high statistical significance. Here, we reanalyze the same set of XMM-Newton data measured on 2008 February 4 with the Weighted-Wavelet Z-transform (WWZ) method. In addition to confirm the previous finding we find the other QPO signal in a separated X-ray emission phase at a confidence level of $\sim 4.1\sigma$. The frequency ratio between these two signals is $\sim 2 : 1$. These two signals also appeared, though at lower significance levels, in XMM-Newton measurements on 2007 May 14 and 2010 September 17, individually. This is the first time to observe two separated transient X-ray QPOs in active galactic nuclei (AGNs), which sheds new light on the physics of accreting supermassive black holes.

PACS numbers: 98.54.Cm, 96.60.tk, 95.85.Nv

I. INTRODUCTION

Active galactic nuclei (AGNs), the most persistent luminous sources of electromagnetic radiation in the universe, are widely believed to be powered by the accretion of material onto supermassive black holes (SMBHs). Narrow-line Seyfert 1 galaxies (NLS1s) serve as a peculiar subclass of AGNs, with common definition based on their optical spectra (a narrow width of the broad Blamer emission lines with FWHM ($H\beta$) $< 2000 \text{ km s}^{-1}$, along with strong optical Fe II lines and weak forbidden lines) [1–3]. Other extreme properties include rapid X-ray variability, near-Eddington accretion rates as well as strong star formation of the host galaxies, indicating a rapidly growing phase of their central black holes [4]. Furthermore, the γ -ray emissions of NLS1s [5, 6] render them a new member of the jetted-AGN family. Therefore, the studies of NLS1s are essential to have a through understanding of the AGN phenomena.

Periodic emissions are well detected in X-ray light curves of Galactic binary systems [7–9] and the periodic variabilities are widely adopted to probe the physics of accretion disk [10]. However, in AGNs, the periodicity is relatively rare. Some detections or evidences for periodic variabilities in optical, X-ray, and/or gamma-ray emission of AGN have been reported in the literature [11–16]. In X-rays, a significant transient QPO has been detected in NLS1 galaxy RE J1034+396 [17]. Recently, the other significant transient QPO signal has been reported in NLS1 galaxy 1H 0707-495 [18]. In this work, we re-analyze the data set adopted by [18] with the Weighted-Wavelet Z-transform method. In addition to confirm previous finding, we find a new QPO signal in the early part of the light-curve with a period cycle of $\sim 8240 \text{ s}$ at the confidence level of $\sim 4.1\sigma$. These two QPO signals, with a frequency ratio of $\sim 2 : 1$, are separated by an intermediate state. Inter-

estingly, in two other observation data sets these signals appeared, though individually and at lower significance levels. Our conclusions are thus further strengthened.

II. OBSERVATION AND DATA ANALYSIS

A. The construction of X-ray light curves

The X-ray Multi-Mirror Mission (XMM-Newton) was launched on December 10th 1999 by European Space Agency's (ESA). *XMM-Newton* carries a set of three X-ray CCD cameras, including two MOS [19] and one PN [20], with an unprecedented large effective area. The NLS1 galaxy 1H 0707-495 had been monitored 15 times over 40 ks with the former three detectors between 2000 January and 2011 February in a full frame imaging mode. The data analysis is performed following the standard procedure in the Science Analysis Software (SAS) with version of 16.0.0 provided by the *XMM-Newton* science operations center¹. The events are extracted from a circle region of interest (ROI) of 40-arcsec radius centered on the position (R.A. = 107.173, dec. = -49.552) of the target in 0.2-10.0 keV with time-bin of 100 s. We exclude the events in periods with high background flaring rates exceeding 0.4 counts/s, and only the good events (the PATTERN ≤ 4 for PN and PATTERN ≤ 12 for MOS) are used in generating light curves. For background, the events are extracted from a source-free circle (without any other source) with the same diameter in the same chip. Then, the correction performed by tool *epiclccorr* has been accomplished, and the pile-up effect is negligible. We combine the three (PN+MOS1+MOS2) background subtracted light curves, and show them in the top panels of Fig.1 and Fig.2; the following analysis is based on these combined light curves.

*Electronic address: jzyan@pmo.ac.cn

†Electronic address: yzf@pmo.ac.cn

¹ <https://www.cosmos.esa.int/web/xmm-newton/sas-threads>

B. The analysis of periodic variability

The wavelet transform is a widely used method for searching the periodic signal in the time series by changing the parameters of wavelets to fit light curves in both time and frequency domains. This method is different from Fourier analysis, which pays attention to a limited time span of data. A key advantage it has over Fourier transforms is temporal resolution: it captures both frequency and location information (location in time). However, this method may yield untrustworthy results because of the local number density of the uneven data points. While a modified version of weighted wavelet Z-transform with a Morlet mother function has been provided in [21], which handles efficiently this problem by rescaling the wavelet function. Therefore, we calculate WWZ power spectrum for light curves. In the II and III panels of Fig.1, we present the color-scaled WWZ power spectrum for the whole light-curve; WWZ power spectral and time-averaged WWZ power spectral for the first and second segment, respectively.

Pan et al. [18] divided the light-curve into two segments (see Fig. 1 therein) and then calculated the power spectrum density (PSD) with Fourier analysis for the second segment. They detected a QPO with a strong peak at $2.6 \pm 0.18 \times 10^{-4}$ Hz (which corresponds to a period of 3800 s). We use the WWZ method to re-analyze the data and surprisingly find two signals, separated by a short intermediate state, at different frequencies (see the panel II of Fig.1). We thus calculate the power spectrum for both segments, respectively. The WWZ powers for the second segment reveal a clearly peak (see the bottom C and D panels of Fig.1), in agreement with Pan et al. [18]. While, in the segment 1, another QPO also appears in the WWZ power and time-averaged WWZ at $1.21 \pm 0.12 \times 10^{-4}$ Hz (see the III A and III B panels of Fig.1).

The uncertainty is evaluated as the means of the half width at half maximum of the fitting with a Gaussian function centered around the maximum time-averaged WWZ power. The maximum time-averaged WWZ power is ~ 14.5 times of the underlying continuum with the false-alarm probability of $\sim 5.0 \times 10^{-7}$. In order to establish a robust significance, we generate the artificial light curves with a simulator [22, 23], and the simulator is based on the power spectral density (PSD) and the probability density function of observed variation. Therefore, the artificial light curves has full properties of statistical and variability as the X-ray flux of the target. For determining the beat-fitting of PSD, we fit the PSD with a power-law function as $P(f) = A \times f^{-\alpha}$, α is the index of the model with the value of 1.3. The detailed information of the method for evaluating of significance level is provided in [14, 17, 22, 24]. In total, we generate $\sim 2 \times 10^6$ light curves. In the III A panel of Fig.1, the 4σ , 3σ and 2σ confidence levels are shown with the red solid, blue dotted-dashed and green dashed curves, respectively.

For revealing the variability of X-ray flux, we fold the light-curve with a tool *efold* provided in HEASOFT Software using the period cycle of 8244.36 s with phase zero corresponding to 318550671.023 s. And the tool is provided in HEASOFT

Software². The folded X-ray light-curve is fitted with a constant model, the reduced $\chi^2/\text{d.o.f}$ is 7875/49, it is shown in the I A panel (i.e., the insert) of Fig.1 with a red dashed-dotted line representing the mean count rate of 7.51 counts/s, which reveals a significant variability of folded light-curve varying with phase. Furthermore, this result confirms the periodic variability again. And error bars in the fold light-curve are calculated from the standard deviation of the mean values of each phase bin. For clarity, we show two period cycles.

We have searched for possible signals in other observation data sets for this source. Interestingly in two observations there are tentative QPO signals (see Fig.2, the left panel is for the measurement on 2010 September 17 and the right panel is for the measurement on 2007 May 14). The confidence levels for signals in the observations on 2007 May 14 and 2010 September 17 are $\sim 3.6\sigma$ (the powers peak at $2.70 \pm 0.24 \times 10^{-4}$ Hz) and $\sim 3.1\sigma$ (the powers peak at $1.21 \pm 0.06 \times 10^{-4}$ Hz), respectively. These periodic cycles are well consistent with those displaying in the emission on 2008 February 4, strongly favoring the transient nature of the QPOs in X-rays of NLS1 galaxies suggested in [17] and [18].

III. SUMMARY AND DISCUSSION

In this work, we have re-analyzed the XMM-Newton observation data of NLS1 galaxy 1H 0707-495. By dividing the X-ray light-curve measured on 2008 February 4 into two segments, we construct the WWZ powers with the WWZ method, respectively. In the power spectrum of segment 2, there is a strong signal peaks at $2.64 \pm 0.09 \times 10^{-4}$ Hz, which confirms the previous detection of QPO at $2.6 \pm 0.18 \times 10^{-4}$ Hz in [18]. Surprisingly, we find a new QPO signal in the power spectrum of segment 1. Such a signal is at $1.21 \pm 0.12 \times 10^{-4}$ Hz with a significance of $\sim 4.1\sigma$ and the root-mean-square (rms) in segment 1 has a fractional variability of $\sim 30\%$ with a mean count rate of 7.5 counts/s. The two QPO signals are separated by an intermediate state in light-curve and the frequency ratio is $1 : 2.14 \pm 0.26$. This is the first time to observe two QPO signals, separated by an intermediate state, in X-ray emission of AGNs. Our conclusion is further supported by the presence of these two signals, though at lower significance levels, in XMM-Newton measurements on 2007 May 14 and 2010 September 17, respectively.

The physical origin of QPO signals in X-ray binaries as well as AGNs is still to be better understood [10, 25]. Nevertheless some models do suggest frequency ratios of $1 : 2 : 3$ and so on. For example, Lai & Tsang [26] studied the global stability of non-axisymmetric p modes (also called inertial-acoustic modes) trapped in the innermost regions of accretion discs around black holes and showed that the lowest-order p modes, with frequencies $\omega \approx 0.6m\Omega_{\text{ISCO}}$ can be overstable due to general relativistic effects, where $m = 1, 2, 3, \dots$ is the azimuthal wavenumber and Ω_{ISCO} is the

² <https://heasarc.gsfc.nasa.gov/docs/software/lheasoft/download.html>

disc rotation frequency at the so-called innermost stable circular orbit (ISCO). They also suggested that overstable non-axisymmetric p modes driven by the corotational instability may account for the high-frequency QPOs observed from a number of BH X-ray binaries in the very high state while the absence of such signals in the soft (thermal) state may result from mode damping due to the radial infall at the ISCO. While in our scenario it is required that different m appeared in different time intervals. We have analyzed the emission properties in segment 1 and segment 2 but did not find significant change. Therefore the physical origin of our phenomena is still a mystery.

Acknowledgments

This work was supported in part by the National Basic Research Program of China (No. 2013CB837000) and the National Key Program for Research and Development (2016YFA0400200), the National Natural Science Foundation of China under grants of No. 11525313 (i.e., the Funds for Distinguished Young Scholars), No. 11573071, No. 11673067, and the Key Laboratory of Astroparticle Physics of Yunnan Province (No. 2016DG006).

-
- [1] Osterbrock, D. E. & Pogge, R. W., *Astrophys. J.*, **297**, 166 (1985)
 - [2] Goodrich, R. W., *Astrophys. J.*, **342**, 224 (1989)
 - [3] Pogge, R. W., *New Astron. Rev.*, **44**, 381 (2000)
 - [4] Komossa, S., *Rev. Mex. Astron. Astrophys. Conference Ser.*, **32**, 86 (2008)
 - [5] Abdo, A. A., Ackermann, M., Ajello, M., et al. *Astrophys. J.*, **699**, 976 (2009)
 - [6] Liao, N.-H., Liang, Y.-F., Weng, S.-S., Gu, M.-F., & Fan, Y.-Z., *arXiv:1510.05584* (2015)
 - [7] Bolton, C.T., *Nature*, **235**, 271 (1972)
 - [8] Ackermann, M., Ajello, M., Ballet, J., et al., *Science*, **335**, 189 (2012)
 - [9] Webster, B.L., & Murdin, P., *Nature*, **235**, 37 (1972)
 - [10] Remillard, R. A., & McClintock, J. E., *Ann. Rev. Astron. Astrophys.*, **44**, 49 (2006)
 - [11] Kidger, M., Takalo, L., & Sillanpaa, A., *Astron. Astrophys.*, **264**, 32, (1992)
 - [12] Valtonen, M. J., Lehto, H. J., Sillanpü, A., et al., *Astrophys. J.*, **646**, 36 (2006)
 - [13] Reis, R. C., Miller, J. M., Reynolds, M. T., et al., *Science*, **337**, 949 (2012)
 - [14] Ackermann, M., Ajello, M., Albert, A., et al., *Astrophys. J. Lett.*, **813**, L41 (2015)
 - [15] Zhang, P.-F., Yan, D.-H., Liao, N.-H., Wang, J.-C., *Astrophys. J.*, **835**, 260 (2017)
 - [16] Covino, S., Sandrinelli, A. & Treves, A., *arXiv:1702.05335v1* (2017)
 - [17] Gierliński, M., Middleton, M., Ward, M., & Done, C., *Nature*, **455**, 369 (2008)
 - [18] Pan, H.-W., Yuan, W.-M., Yao, S., et al., *Astrophys. J. Lett.*, **819**, L19 (2016)
 - [19] Turner, M. J. L., Abbey, A., Arnaud, M., et al., *Astron. Astrophys.*, **365**, L27 (2001)
 - [20] Strüder, L., Briel, U., Dennerl, K., et al., *Astron. Astrophys.*, **365**, L18 (2001)
 - [21] Foster G., *AJ*, **112**, 1709 (1996)
 - [22] Emmanoulopoulos D., McHardy I. M., Papadakis I. E., *Mon. Not. R. Astron. Soc.*, **433**, 907 (2013)
 - [23] Timmer, J., & Koenig, M., *Astron. Astrophys.*, **300**, 707 (1995)
 - [24] Bhatta, G., Zola, S., Stawarz, Ł., et al., *Astrophys. J.*, **832**, 47 (2016)
 - [25] Li, L.-X., & Narayan, R., *Astrophys. J.*, **601**, 414 (2004)
 - [26] Lai, D., & Tsang, D., *Mon. Not. R. Astron. Soc.*, **393**, 979 (2009)

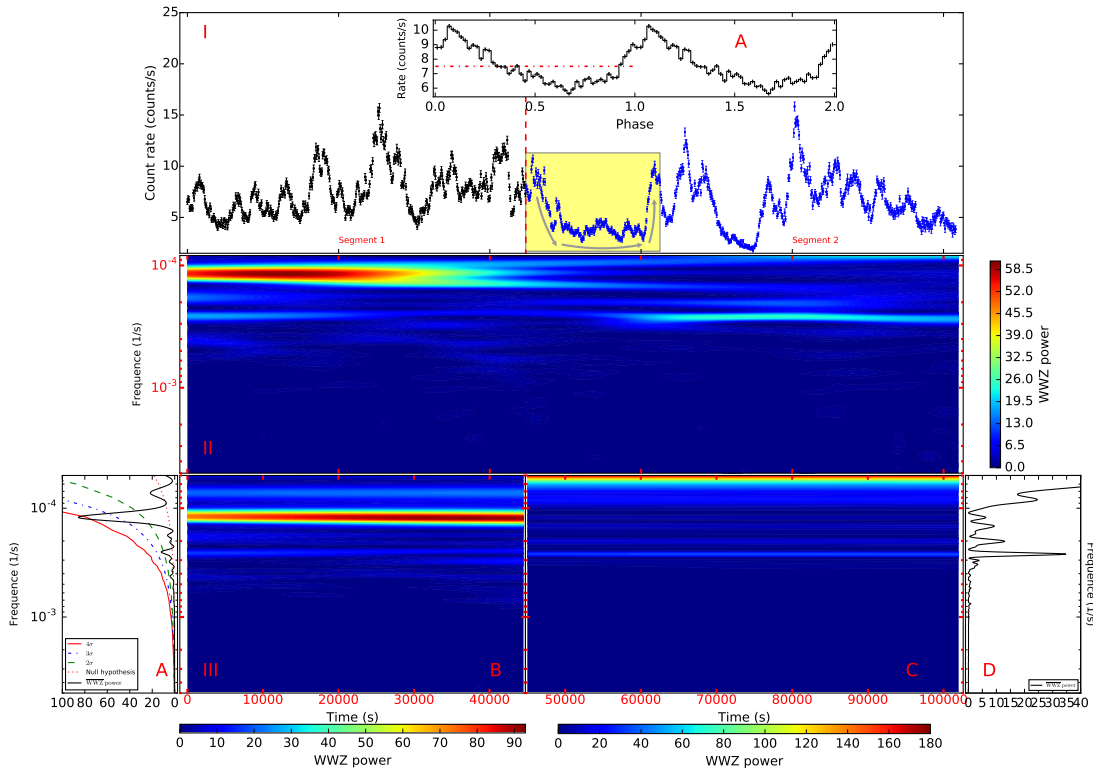


FIG. 1: Panel I: The *XMM-Newton* light-curve of target in 0.2-10 keV with 100-s per bin is observed on 2008 February 4 (Obs ID:0511580401), the two segments are separated with a red dashed line. And the pulse shape (the folded X-ray light-curve for segment 1) with a period cycle of 8244.36 s is shown in the inset A panel (two cycles are shown). The yellow box represents the intermediate state. Panel II: The 2D plane contour plot of the WWZ power of the whole X-ray light-curve with color contour filled. The color-bar in the middle right panel is scaled with WWZ power value. Panel III: in the A part, the curves of confidence levels of 4σ , 3σ and 2σ are shown with red solid, blue dotted-dashed and green dashed lines, respectively. The black solid line represents time-averaged WWZ power. The red dotted line represents the true power distribution under our null hypothesis. The B part presents the contour plot of the WWZ power of segment 1. The C part is the contour plot of the WWZ power of segment 2. The D part gives the time-averaged WWZ power of segment 2.

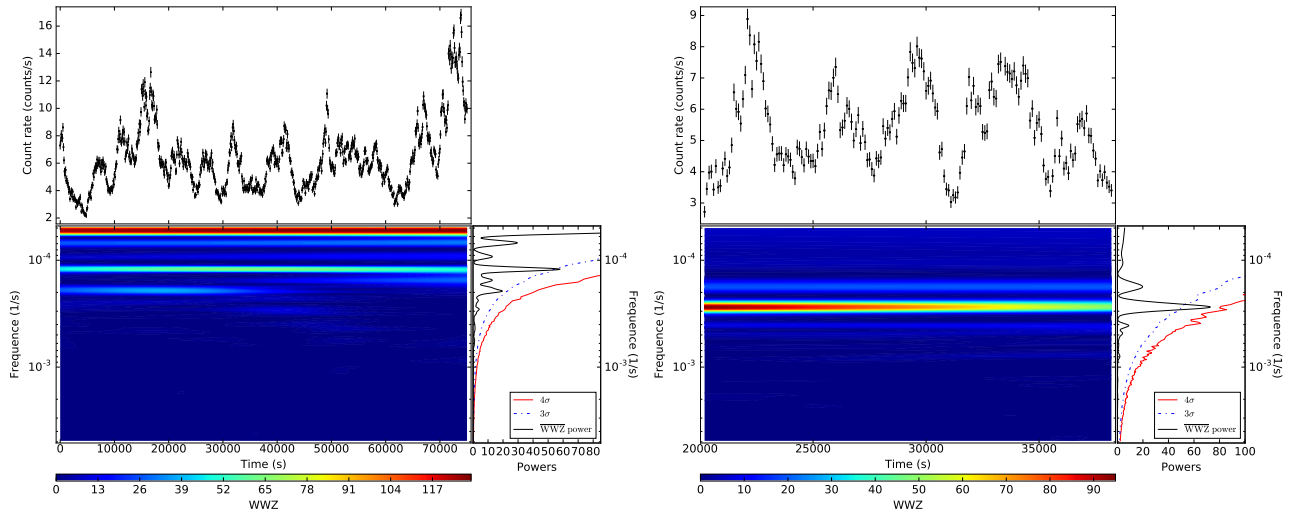


FIG. 2: The upper panels are the *XMM-Newton* light-curve of target in 0.2-10 keV with 100-s per bin. The lower left panel is the contour plot of the WWZ power of upper light-curve. The lower right panel: the time-averaged WWZ power. The left and right images are the observations of *XMM-Newton* on 2010 September 17 (Obs ID: 0653510501) and on 2007 May 14 (Obs ID: 0506200301), respectively.